

Rock Types and Reservoir Characteristics of Shahejie Formation Marl in Shulu Sag, Jizhong Depression, Bohai Bay Basin

Jingwei Cui^{1,2,3*}, Xuanjun Yuan^{1,2,3}, Songtao Wu^{1,2,3}, Ruifeng Zhang⁴, Song Jin⁵, Yang Li¹


1. Research Institute of Petroleum Exploration and Development, CNPC, Beijing 100083, China

2. Key Laboratory of Oil and Gas Reservoirs, CNPC, Beijing 100083, China

3. National Energy Tight Oil and Gas R&D Center, Beijing 100083, China

4. Exploration Department of PetroChina Huabei Company, Renqiu 062552, China

5. Hebei Institute of Geological Survey, Shijiazhuang 050081, China

 Jingwei Cui: <https://orcid.org/0000-0002-8361-9284>

ABSTRACT: Due to the complicated lithology in the E₃ Member of the Shahejie Formation in the Shulu sag, Jizhong depression, it is difficult to classify the rock types and characterize the reservoirs at the marl intervals. In this paper, a four-element classification method has been proposed, and seven rock types have been identified by analyzing the mineral composition. The primary rock types are medium-high organic carbonate rocks and medium-high organic shaly-siliceous carbonate rocks. With the methods of field emission scanning electron microscopy, high-pressure mercury intrusion, nitrogen adsorption, and nano-CT, four types of reservoir spaces have been identified, including intra-granular pores, inter-granular pores (inter-crystalline pores), organic pores, and micro-fractures. By combining the method of high-pressure mercury intrusion with the method of the nitrogen adsorption, the porosity of the marl has been measured, ranging from 0.73% to 5.39%. The distribution of the pore sizes is bimodal, and the pore types are dominated by micron pores. Through this study, it has been concluded that the sag area to the east of Well ST1H is the favorable area for the development of self-sourced and self-reservoired shale oil. According to the results of geochemical and reservoir analysis, the III Oil Group may have sweet spot layers.

KEY WORDS: marl, shale oil play, rock types, tight reservoir, Bohai Bay Basin.

0 INTRODUCTION

In the united states, many unconventional oil production zones have been established in marine shale plays in recent years, such as Eagle Ford, Wolfcamp, and Bakken shale areas, and the unconventional oil production has accounted for more than 50% of the total US crude oil (Cui et al., 2019; EIA, 2019). In fact, in North America, the shales have been divided further into three types according to the rock mineral composition, including calcareous shale, siliceous shale and clay-rich shale (Cui J W et al., 2015). Previous studies have found that the type of marl in the Shulu sag is a kind of fine-grained mudstone, with horizontal beddings. The rock compositions are *in-situ* sediments (dark mud and well-crystallized gray matters) and terrestrial sediments (carbonate, feldspar, quartz of different particle sizes), being mixed rocks and mixed sediments (Liang et al., 2007; Yang and Sha, 1990). In the E₃¹ of the Shahejie Formation in the Shulu

sag, marl and conglomerate are well developed, which are generally called marl (Zhao et al., 2014).

In recent years, at home and abroad, important progresses have been made in the description, classification and sedimentary diagenesis analysis of the fine sediments (Chen, 2016; Ma et al., 2016; Zhou, 2016; Lazar et al. 2015; Yan, 2015; Jiang, 2013), especially in the study of tight reservoirs, including planar identification of pores with the methods of field emission scanning electron microscope (FE-SEM) after cutting by argon ion, and digital core analysis through CT for 3D reconstruction of pore structures, as well as analysis of connectivity and distribution of pore sizes (Li et al., 2019; Zhu et al., 2013; Clarkson et al., 2012; Loucks et al., 2009). In addition, nitrogen adsorption method has been used to evaluate quantitatively the pore structures of tight rocks such as shale (Cao et al., 2016; Clarkson et al., 2013, 2012; Sondergeld et al., 2010). In the Shulu sag, core samples from wells ShuTan 1H and ST-3 have been taken for basic studies, and a lot of studies have been carried out on analysis of the rock types, reservoir development, controlling factors for the sweet spots of the tight oil reservoirs. Especially, the marls have been classified into lamellar and massive marls (Fu et al., 2019; Jiang et al., 2019; Tang et al., 2018; Li et al., 2016; Cui Z Q et al., 2015; Han et al., 2015; Zhang et al.,

*Corresponding author: jingwei.cui@126.com

© China University of Geosciences (Wuhan) and Springer-Verlag GmbH Germany, Part of Springer Nature 2021

Manuscript received April 17, 2020.

Manuscript accepted September 6, 2020.

2015; Zhao et al., 2015; Song et al., 2013; Qiu et al., 2006).

In this study, the core samples from the important exploration well (Well ST1H) have been analyzed for a detailed comprehensive study of mineral composition, the geochemical characteristics of the source rocks and the reservoir properties in order to gain new understandings in the following three aspects. Firstly, systematical evaluation has been conducted on the mineral composition and geochemical characteristics of the Shahejie Formation marl, and subdivision of the marl types has been done with the core samples from the vertical Well ST1H; secondly, quantitative and qualitative reservoir characterization has been made, characterization of 2D and 3D reservoir features has been carried out, and the control factors for reservoir development has been analyzed.

1 GEOLOGICAL SETTING AND EXPERIMENTS

1.1 Geological Setting

The Shulu sag is located in the southern part of the Jizhong

depression, being a half-graben developed on Paleozoic basement, extending in northeast direction, and faulted in the east and overlapped in the west, with an exploration area of more than 700 km². At present, five oil-bearing series (O, C-P, Es₁, Es₂ and Es₃) have been discovered, with many types of reservoirs, including sandstones, conglomerates, marls, carbonate reservoirs and other types (Cui Z Q et al., 2015; Zhao et al., 2015). The Paleogene has three reservoir combinations, namely Es₁ sandstone, Es₂ and Es₃ sandstone and Es₃ marl in descending order. During the early depositional period of Es₃ Member of Shahejie Formation of Paleogene, two paleo-uplifts (Jingqiu and Tierzhuang) and marginal faults divided the Shulu Basin into three water bodies (southern, central, and northern), which were not fully communicated, and gradually became salty from north to south (Jiang et al., 2019; Zhao et al., 2015) (Fig. 1a).

The Es₃ Member covers directly on the Paleozoic basement, characterized by thick in the east and thin in the west, with the maximum thickness over 1 200 m, of which the maximum

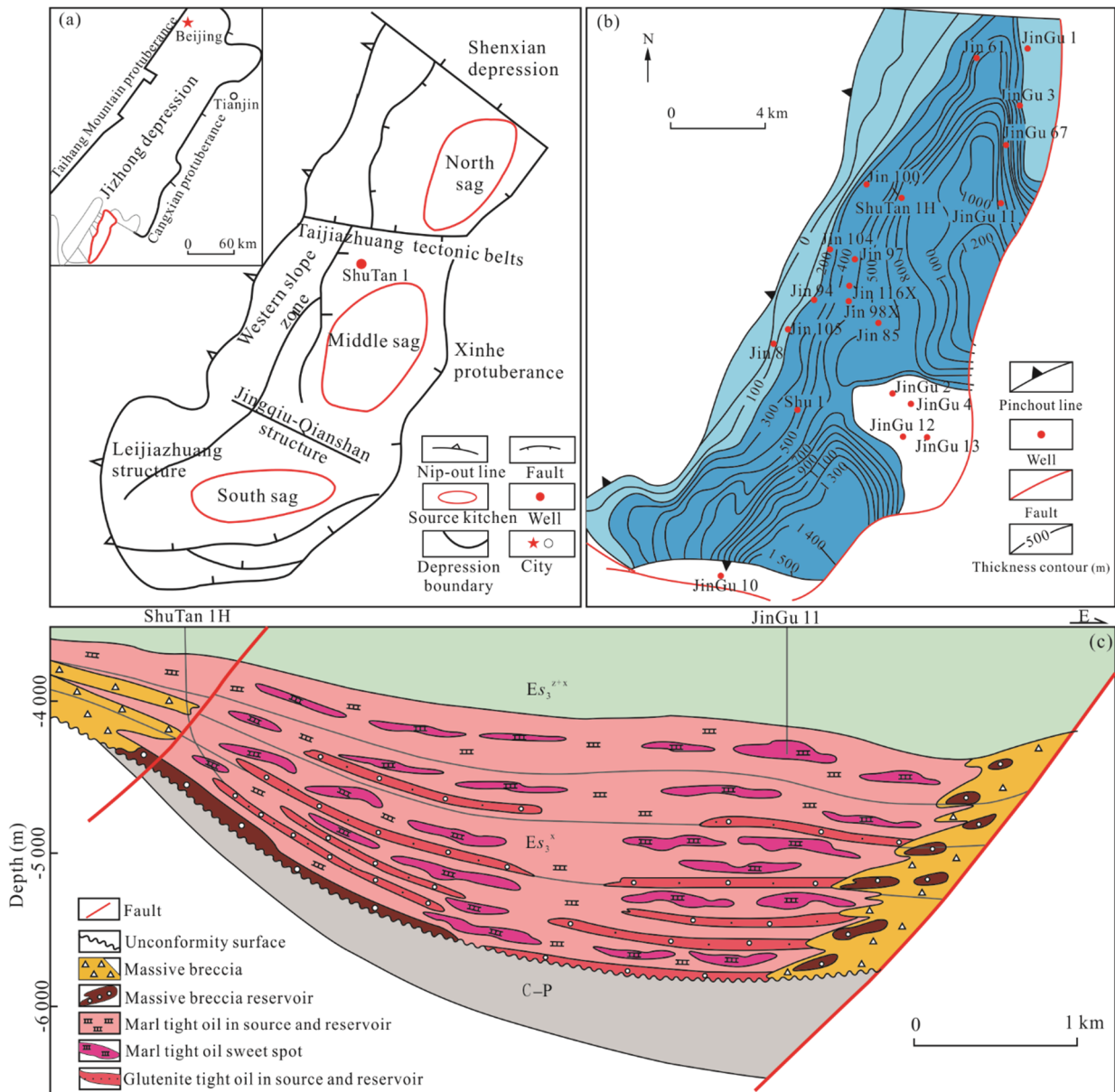


Figure 1. Geological structure and thickness distribution of marl in Shulu sag (adapted from Zhao et al., 2015).

thickness of conglomerate is 520 m, and the maximum thickness of marl is 403 m. Carbonate rock is developed on the steep and gentle slopes, and thick marl is developed in the deep low part of the Shulu sag (Fig. 1b). The thick marl is more than 200 km² in area, with burial deep over 3 000 m. According to 3D seismic data, Es₃¹ sub-member can be divided into five third-order sequences and four oil groups, of which the five third-order sequences are SQ1, SQ2, SQ3, SQ4 and SQ5 in ascending order, with SQ1, SQ2, and SQ3 corresponding to oil groups IV, III, and II, respectively, SQ4 and SQ5 corresponding to Oil Group I (Han et al., 2015; Zhao et al., 2015) (Fig. 1c).

1.2 Samples and Experiments

In 2013, the micro-reservoir evaluation of the marl in Well ST1 was conducted, and the samples from Es₃¹ marl in oil groups III and II were collected. The sample information is shown in Table 1.

The analysis and testing conditions are described in detail as follows.

X-ray diffraction (XRD) analysis: The test instrument is a TTR type diffractometer (Rigaku Electric Co., Ltd.). This analysis was carried out with the powder pressed method (300 mesh). The mass percentage of each mineral was analyzed using a software, with the K value of international standard sample as a reference. To analyze the composition of the clay minerals, the samples were extracted with the suspension method, and the prepared orientation plate was air-dried at room temperature and

then tested. The samples were saturated with ethylene glycol for 8 h at 60 °C, and then were heated at 550 °C for 2.5 h. The obtained high-temperature plate was then tested, and the mass percentage of each clay mineral was calculated using a software.

The TOC analysis was conducted with the LCO CS230 carbon and sulfur analyzer. Following the National Standard GB/T 19145-2003, the analysis was conducted in four steps. The first step was to weigh the sample powder of about 10 mg with the electronic balance, and put it into the porous ceramic crucible (which was heated for 2 h in the muffle furnace at 1 000 °C). The second step was to add a sufficient amount of 12.5% hydrochloride (HCL) and heat it on the electric heating plate at 60 °C for two hours until the reaction was complete. The third step was to put the crucible into the filter container, and add distilled water every half-hour period and rinse for three days at one-hour intervals. The fourth step was to dry the crucible in a furnace at 60 °C, and then to test the TOC content after cooling.

Scanning electron microscope (SEM) analysis: The test instrument is Quanta 650F thermal field emission SEM (FEI, USA). The samples were cut into small pieces, and polished into pieces with the size of 1 cm×1 cm×1 cm using P50 coarse and P500 fine sandpapers. The observed surface must be the natural section (and not the polished). The ready-made rock fragments were glued to the sample pile using a conductive adhesive, and then were kept for 1 day until the adhesive was dried completely. The samples were then coated with gold and observed under SEM.

Table 1 Sample information

No.	Depth (m)	Formation	Lithology	Barrels of cores	Oil group	Sequence	System tract
ST-1	3 940.5	Es ₃	Marl	1	II	SQ3	LST
ST-3	3 960.3	Es ₃	Marl	2	II	SQ3	LST
ST-8	3 970.3	Es ₃	Marl	4	II	SQ3	LST
ST-10	3 973.2	Es ₃	Marl	4	II	SQ3	LST
ST-13	3 974.2	Es ₃	Marl	5	II	SQ3	LST
ST-14	3 976.5	Es ₃	Marl	5	II	SQ3	LST
ST-16	3 979.1	Es ₃	Marl	6	II	SQ3	LST
ST-18	3 984.7	Es ₃	Marl	7	II	SQ3	LST
ST-20	3 989.9	Es ₃	Marl	8	II	SQ3	LST
ST-24	3 994.5	Es ₃	Marl	8	II	SQ3	LST
ST-26	4 033.7	Es ₃	Marl	9	II	SQ3	LST
ST-27	4 036.0	Es ₃	Marl	9	II	SQ3	LST
ST-30	4 074.0	Es ₃	Marl	10	II	SQ3	HST
ST-31	4 074.9	Es ₃	Marl	10	II	SQ3	HST
ST-33	4 077.4	Es ₃	Marl	10	II	SQ3	HST
ST-34	4 077.5	Es ₃	Marl	11	II	SQ3	HST
ST-36	4 079.0	Es ₃	Marl	11	II	SQ3	HST
ST-38	4 082.1	Es ₃	Marl	11	II	SQ3	HST
ST-41	4 084.5	Es ₃	Marl	12	II	SQ3	HST
ST-43	4 087.7	Es ₃	Marl	12	II	SQ3	HST
ST-45	4 204.8	Es ₃	Marl	13	III	SQ2	TST
ST-47	4 206.3	Es ₃	Marl	13	III	SQ2	TST
ST-48	4 208.0	Es ₃	Marl	13	III	SQ2	TST
ST-50	4 211.5	Es ₃	Marl	13	III	SQ2	TST

The mercury intrusion analysis was conducted using a Quantachrome automatic porosity analyzer, with incremented pressure values of 10 MPa (up to 210 MPa). The N₂ adsorption experiment was carried out on Malvern ASAP 2020, being search-level ultra-performance full-auto gas adsorption system (which can work for a pore size of 1.7–300 nm). Before testing, the samples were dried at 110 °C under vacuum for 24 h to remove moisture, and cooled to room temperature (~23 °C) in a desiccator with a relative humidity of less than 10%. The PSD (Pore size distribution) was determined by the Washburn equation (Washburn, 1921), with a contact angle of 140° and a surface tension of 485 dyne/cm (Gregg and Sing, 1982).

An Ultra XRM-L200 microscope was used for Nano CT. The testing process involved sample preparation, CT scanning, image reconstruction, material phase definition (including denoising and segmentation), 3D model reconstruction, and calculation of parameters such as porosity. The most important step was definition of material phase. That is to say, to determine different materials according to the gray value image, and then set parameters to segment. An XM Controller module was used for sample scanning. The exposure time was set to 1 s. Conducted imaging with the continuous imaging mode, tuned finely the X-axis and the Y-axis to move the target to the center of the field of view, then tuned finely the Z-axis, and set the Z-axis down 200 μm. Stopped image acquisition and moved the sample out of the field of view. AXM Reconstruction module was used for data processing to reconstruct the 3D structure.

2 EXPERIMENTAL RESULTS

2.1 Rock Mineral Composition and Total Organic Matter Content

Through analysis of the composition of whole rock and clay minerals, it has been found that the mineral composition of the marl samples is dominated by calcite and dolomite (42.2% to 88.6% and 1.8% to 50.9%, respectively). Calcite and dolomite account for 70% to 95% of the whole rock, respectively. The marl samples are quite different from the ST-1 mudstone sample (3 940.5 m), which is characterized by clay as the primary composition (43%, Fig. 2a). The average content of the quartz in the marl samples is 6.4% (ranging from 2% to 12%), which is much lower than the quartz content (20%) in the ST-1 mudstone samples (3 940.5 m). The clay content in the marl samples generally ranges from 2.1% to 17.4%, with an average of 9.5%. The pyrite content ranges from 0 to 2.3%. Most of the samples do not contain potassium feldspar and plagioclase. The composition of the clay minerals in all samples is mainly the mixed layer of illite and montmorillonite, with content ranging from 59% to 87%, of which the montmorillonite mixing ratio ranges from 5% to 30%, and illite and kaolinite range from 10% to 24% and 0 to 24%, respectively (Fig. 2b). It is worth noticing that chlorite was detected only in the ST-1 sample (3 940.5 m), which may reveal the change in physical and chemical properties during diagenesis of this sample (Zhao and He, 2012).

Through organic geochemical analysis of core samples from Well ST-1, it has been found that the TOC of the E₃¹ marl has changed greatly in vertical, and the lacustrine invasion tract

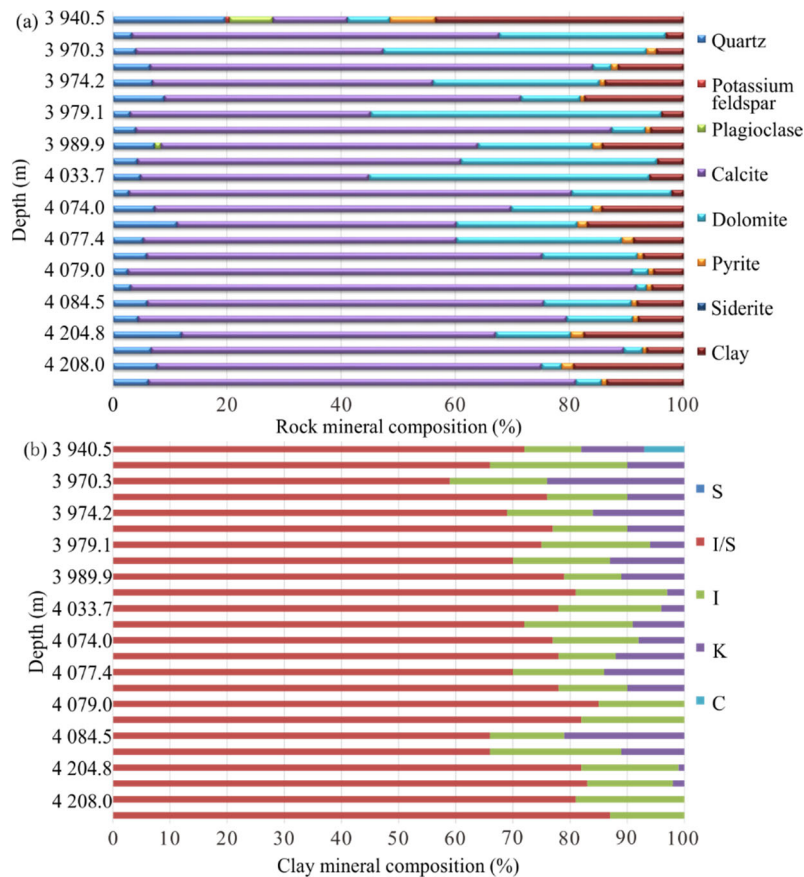


Figure 2. (a) Rock composition of Shahejie samples; (b) composition of clay minerals in samples. S. Montmorillonite ; I. illite; K. kaolinite; C. chlorite.

is the main horizon where the source rocks are well developed in the Shulu sag. Samples with TOC<1.0% account for 21%, 1.0%<TOC<2.0% account for 50%, 2.0%<TOC<4.0% account for 25%. This is comparable with the surrounding wells and their test results (Han et al., 2015; Zhao et al., 2014; Song et al., 2013).

2.2 Reservoirs Characteristics

2.2.1 Pore types

A lot of work has been done on the study of the planar microscopic characteristics of shale reservoirs at home and abroad, using high-resolution FESEM as the primary method. However, at the stage of preparing shale samples, the best method is using argon ion to polish. Loucks et al. (2009) suggested that the shales could be divided into three types, including organic pores, inter-granular pores, and inter-crystalline pores, with no fractures. By observation with FESEM method, it is believed that samples from Well ST1H mainly have micro-nano pores and throats, which are divided into inter-granular pores (inter-crystalline pores), intra-granular pores and

micro-fractures. The inter-granular pores (inter-crystalline pores) include calcite inter-granular pores, clay inter-granular pores, and pyrite inter-granular pores (Figs. 3a, 3c, 3e, 3f), mainly elongated, curved and irregular in shape, and the sizes of micro-pores range from 100 to 500 nm. Micron pores are well developed. The intra-granular pores include organic pores (Figs. 3d, 3j), calcite intra-granular pores (Fig. 4k), and dolomite intra-granular pores (Fig. 3h), mainly round and elongated in shape, being densely distributed, ranging 50 to 400 nm in sizes. Locally, there are nano-scale intra-granular fractures, inter-granular fractures, and organic edge fractures (Fig. 3d), about 200 nm in width (Figs. 3b, 3i, 3l).

2.2.2 Porosity and distribution of pore sizes

Many methods such as high-pressure mercury intrusion, nitrogen adsorption, plane porosity statistics and CT have been used to analyze tight reservoirs (Cui et al., 2019; Zhu et al., 2013). The high-pressure mercury intrusion experiments (at the maximum pressure 210 Mpa) indicated that the Es₃¹ marl has poor physical properties, generally, with the porosity ranging

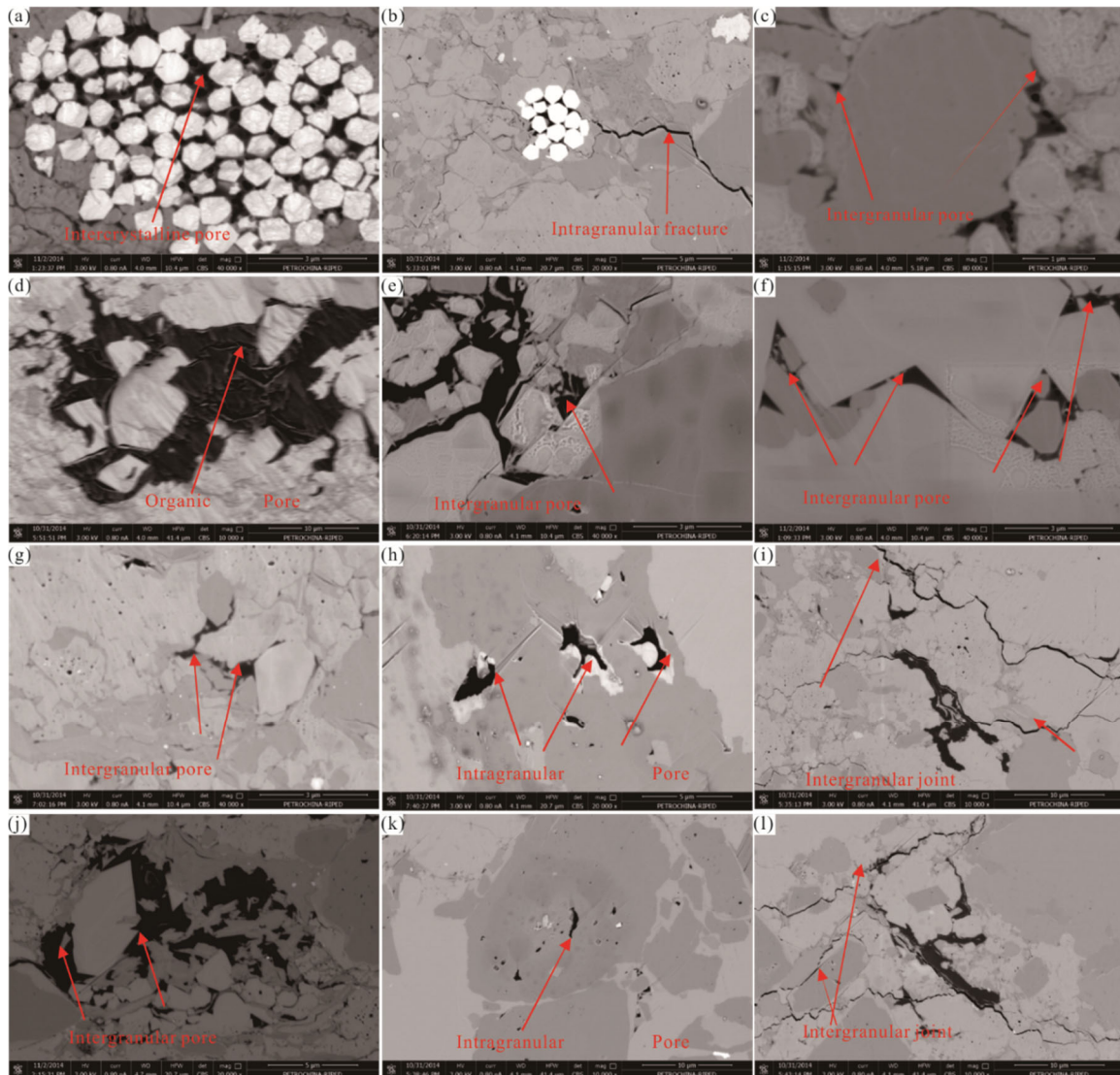


Figure 3. SEM images showing the typical pore types of marl in Well ST1H. (a), (b), (d), (k), (i) Sample ST-3, depth 3 960.3 m; (c), (e), (g) Sample ST-14, depth 3 976.5 m; (h) Sample ST-26, depth 4 033.7 m; (f) Sample ST-34, depth 4 077.5 m.

from 0.36% to 1.99%, with an average of 1.27%. The permeability is less than $0.04 \times 10^{-3} \mu\text{m}^2$, and the permeability of fractured samples is $13.5 \times 10^{-3} \mu\text{m}^2$. The marl reservoirs in Well ST1H are unconventional reservoirs, with different distribution of pore throats. The pore throats of the samples are mainly concentrated above $1 \mu\text{m}$; in some samples, such as ST-1, ST-8 and ST-10, the micro-pore throats below $0.1 \mu\text{m}$ have been locally detected; in the samples from ST-16, 50 to 150 nm micro-pore throats have been detected (Fig. 4). However, the results of SEM observation indicate that tight oil accumulated near source, and the effective reservoir space was mainly connected pores; while the shale oils are self-sourced and self-reservoired, and isolated intra-granular pores may be potentially effective spaces.

Nitrogen adsorption results are usually used to evaluate the structure, specific surface area, average size, and specific volume of mesopores (2–50 nm) in shale (Schmitt et al., 2013). For the Es_3^1 marl samples, the specific surface area ranges from

0.4 to $0.8 \text{ m}^2/\text{g}$, with an average of $0.54 \text{ m}^2/\text{g}$. The BJH pore volume ranges from 0.1 to $0.2 \text{ mL}/100 \text{ g}$, with an average of $0.14 \text{ mL}/100 \text{ g}$. For the lime mudstone samples from ST-1, the specific surface area is $5.7 \text{ m}^2/\text{g}$, and the BJH pore volume is $1.6 \text{ mL}/100 \text{ g}$. The specific surface area and specific pore volume of the marl samples are much smaller than those of the clay-rich shale samples (Clarkson et al., 2013). The BJH pore volume and specific surface area of the ST-1 lime mudstone samples are much higher than the marl samples due to the higher clay content (Fig. 2). In addition, the results of nitrogen adsorption reveal that the distribution style of the pore sizes ranging from 2 to 100 nm is similar, with a relatively high value ranging from 4 to 12 nm (Fig. 5).

3 DISCUSSION

3.1 Classification Scheme of Rock Types

Generally, rock classification is mainly based on grain size

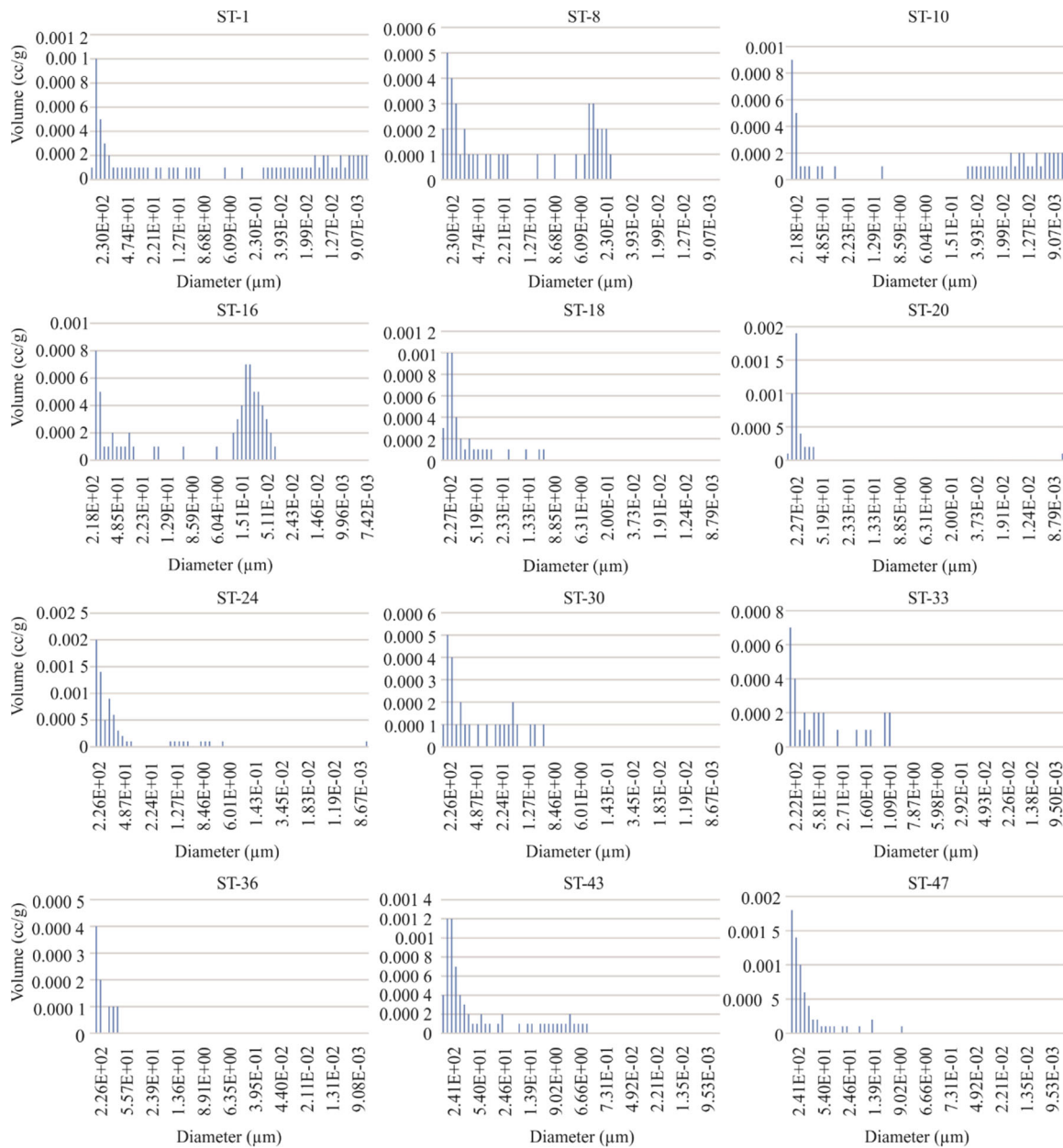


Figure 4. Pore size distribution of the samples detected by mercury intrusion.

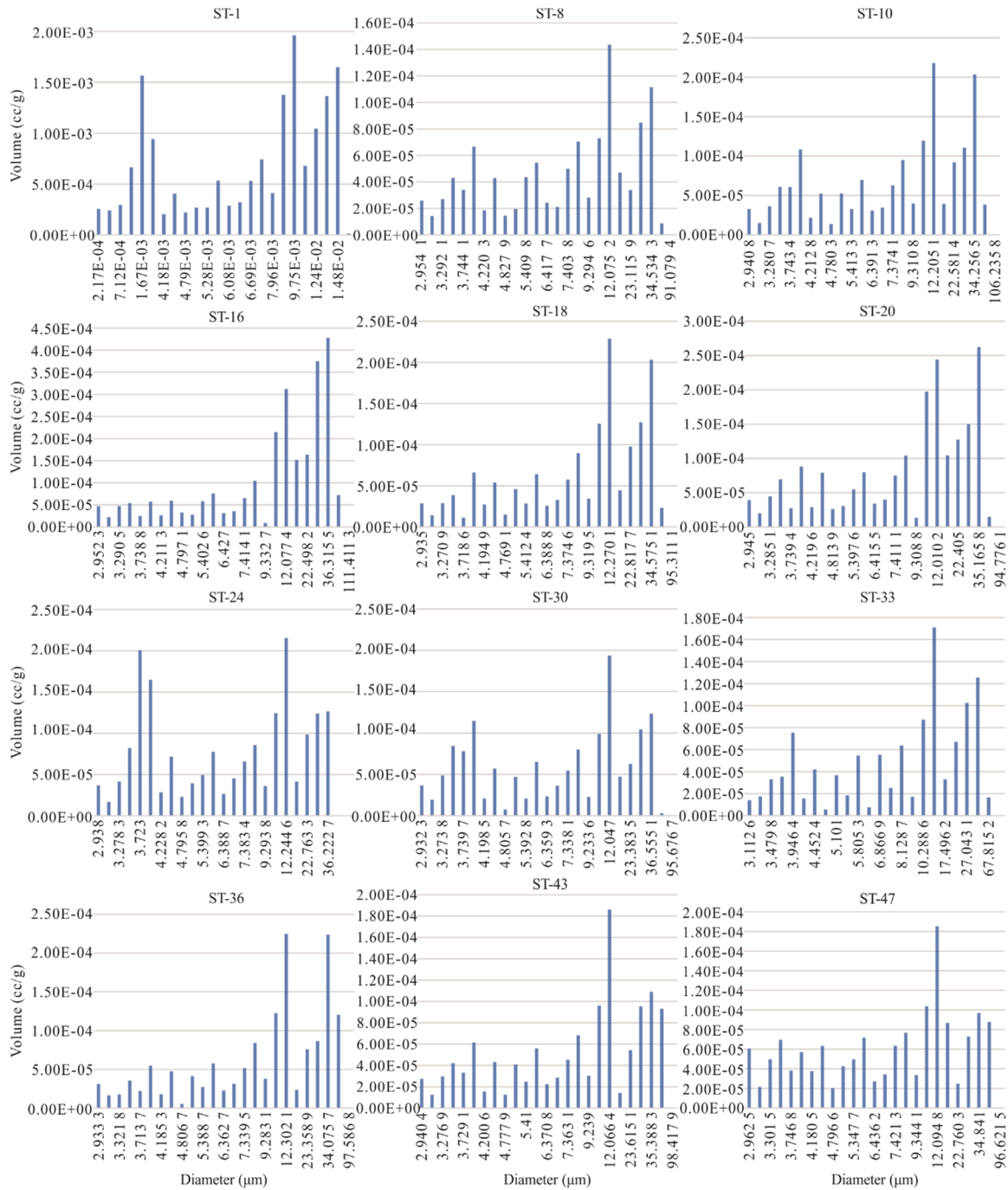


Figure 5. Pore size distribution of the samples tested by nitrogen absorption.

and rock composition. However, with the exploration of shale oil and gas, the organic matter of fine-grained sedimentary rock has become an important evaluation parameter (Lazar et al., 2015; Jiang et al., 2013). The marl is characterized by being self-sourced and self-reservoired, with high TOC. Based on the previous classification of rock types, a four-element method has been proposed to name the Es₃¹ marl, namely siliceous content (quartz+feldspar), calcium content (calcite+dolomite), clay content (clay) and organic matter content (TOC). The parameters are mainly based on the related references (Chen, 2016; Ma et al., 2016; Zhou, 2016; Lazar et al., 2015; Yan, 2015; Jiang et al., 2013). Among them, the TOC evaluation value was modified according to the evaluation criteria for source rock, that is,

0.5%≤TOC<1% is classified as low organic matter, 1.0%≤TOC<2% as medium organic matter, 2.0%≤TOC<4% as high organic matter, and 4.0%≤ TOC as rich organic matter (Fig. 6).

In the Es₃¹ marl of the Shahejie Formation, several types of TOC have been identified, including low organic matter in carbonate rocks, mixed claystone and sandstone; medium organic matter in claystone and clay siliceous carbonate rock; high organic matter in carbonate rocks and clay siliceous carbonate rocks; and rich organic matter in carbonate rocks (Fig. 6). Among them, the medium-high carbonate rock is dominant. Only in ST-1, the organic matter is low in mixed claystones and sandstones. In ST-33, the organic matter is rich in carbonate rocks. This multi-level classification can be realized by

combination of petrophysical plates and neural network methods, especially the preprocessing of primary components, to achieve effective prediction of rock types using geophysical methods such as well logging data (Ma et al., 2016). As an important brittle mineral, carbonate rock is easy to be fractured. According to the equation of shale brittleness index (BI), Jarvie et al. (2007) also believed that the higher the quartz and calcium content, the greater the brittleness.

In fact, in the United States, most of oil and gas producing shales are not composed of more than 50% clay, but are composed of traditional shales and fine-grained biosilicon or carbonates with organic matter. These rocks are more accurately classified into argillaceous limestones, or china stones or wacke limestones with kerogen. It can be seen from the distribution of the samples that the medium-high organic carbonate rocks are dominant. The statistical data reveal that the proportion of the medium-high organic carbonate rocks is over 80%. The Oil Group III is mainly composite by organic high carbonate rocks, while the rest is medium organic carbonate rocks.

3.2 Oil Occurrence and Effectiveness of Pores

Oils in the marl in Well ST1H mainly occurred as thin films on the surfaces of pores and particles (Figs. 7a and 7b). In the calcite dissolved pores, oils mainly occurred as thin films which are connected to each other (Fig. 7c); in the pyrite inter-granular pores, oils were enriched and mainly occurred as thin films. It should be noted that there are small droplets of crude oil in the intra-pores of marl calcite particles, which can only be determined by morphology analysis because the droplet pores

are nanometer scale, and below the detection limit of energy spectrum (Figs. 7d, 7e, 7f).

In this study, based on mercury intrusion data, the combination of the pore volume from mercury intrusion (throats >0.1 μm) and that from nitrogen adsorption (throats <0.1 μm) is taken as the actual pore volume of the samples (Table 2) for reservoir evaluation. At present, for evaluation of the pore distribution of all pore sizes of tight reservoirs, the pore fusion method has been widely used in the world. That is, the pore of the first cross-point (POC) is determined by the nitrogen adsorption curve and the mercury intrusion curve. Pores smaller than the POC are based on nitrogen adsorption data, and pores larger than the POC are based on mercury intrusion data (Cao et al., 2016; Clarkson et al., 2013, 2012; Schmitt et al., 2013). However, this method is not based on strict mathematics (Clarkson et al., 2012). Because nano-scale throats (<0.1 μm) detected by mercury intrusion experiments were only found in a small number of samples such as ST-16, it is believed that most nano-scale throats (<0.1 μm) are isolated.

3.3 Sweet Spot Intervals of Marl Shale Oil

Production is an important indicator of sweet spots, which is influenced by many factors, such as fracture characteristics, completion indicators and reservoir quality. The related oil properties include reservoir physical properties, gas-to-oil ratio (GOR), TOC, maturity, pay thickness, and formation pressure (Cui J W et al., 2015). According to the exploration experience of marine shale oil at home and abroad, the key parameters of sweet spots of marine shale oil are as follows (Cui J W et al.,

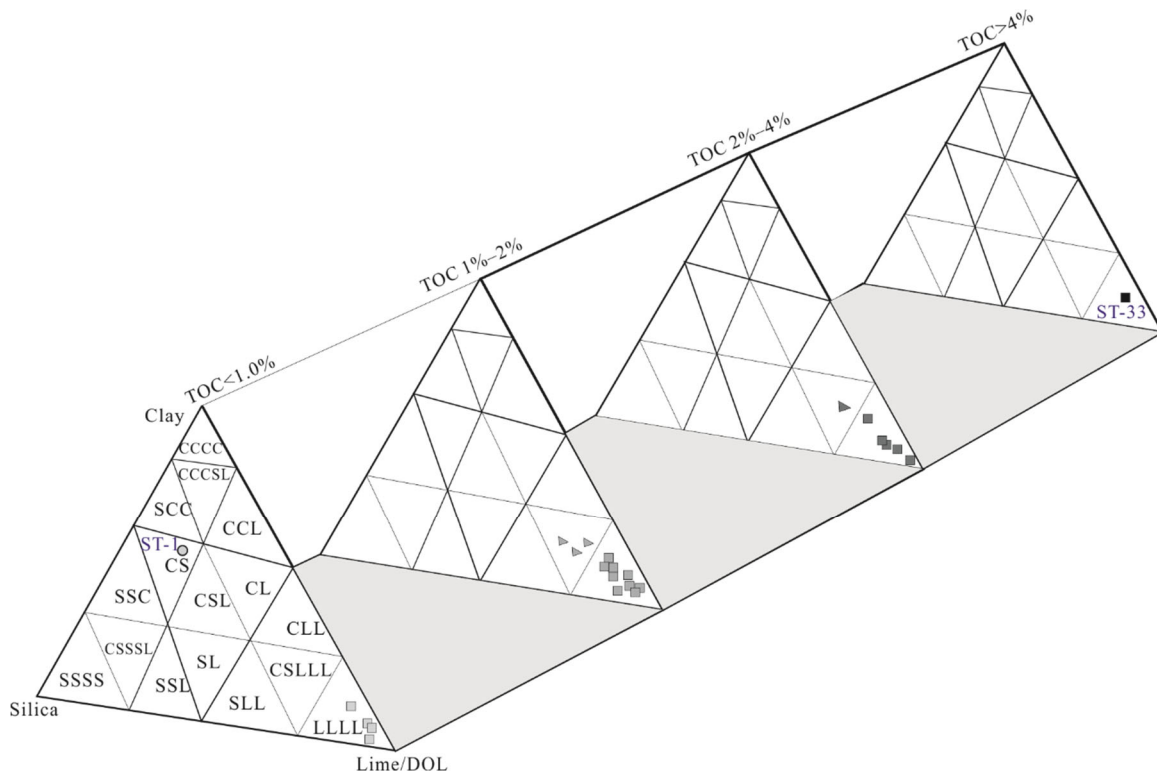


Figure 6. Classification chart of rock types based on mineral composition. CCCC. Claystone; CCCSL. calcareous siliceous claystone; SCC. siliceous claystone; CS. mixed claystone and sandstone; SSC. clayey sandstone; CSSSL. clayey calcareous sandstone; SSSS. sandstone; CCL. calcareous claystone; CL. mixed claystone and carbonate rock; CSL. three-component mixed mudstone; SL. mixed sandstone and carbonate rock; SSL. calcareous sandstone; CLL. clayey carbonate rock; CSLLL. clay siliceous carbonate rock; SLL. siliceous carbonate rock; LLLL. carbonate rock.

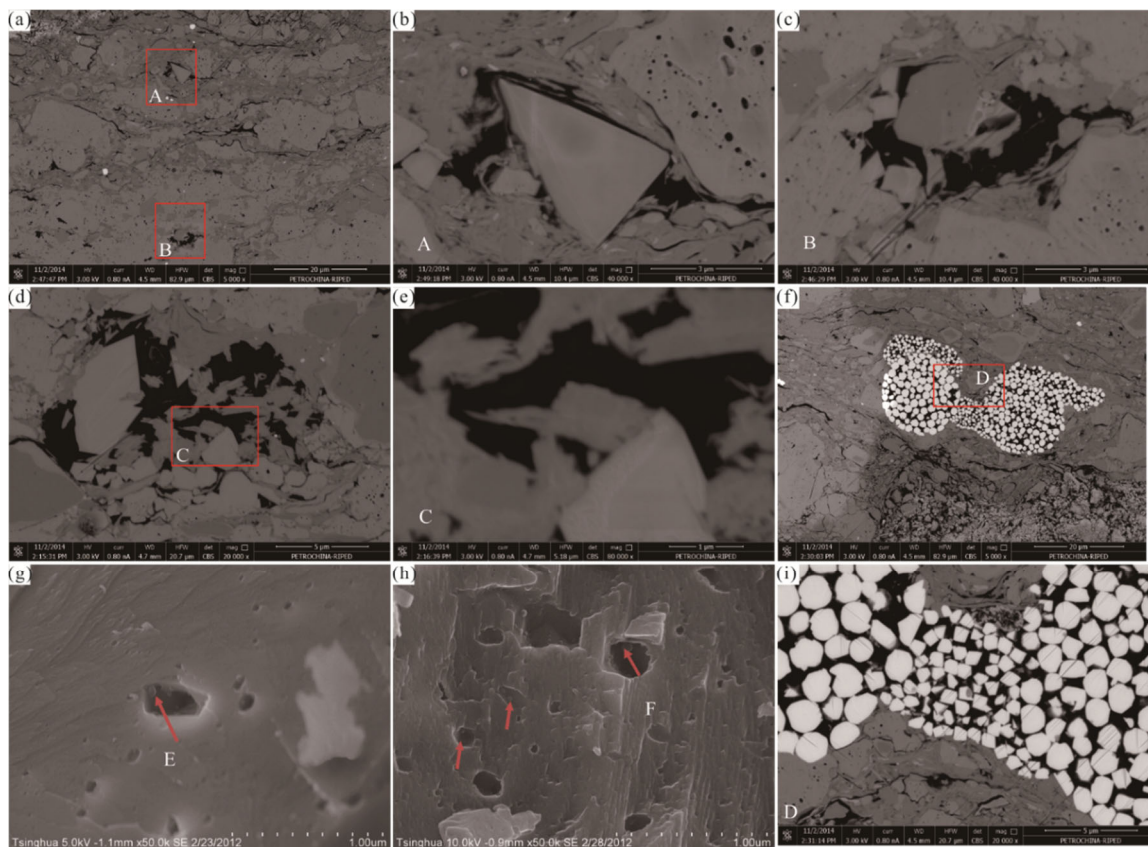


Figure 7. Oil occurrence in marl in Well ST1H. (a) ST-50, 4 211.5 m; (b) an enlarged view of area A in picture (a) shows the thin film of crude oil in the pores at the edge of the particles; (c) an enlarged view of area B in Picture (a) shows the thin film of crude oil in the pores at the edge of the particles; (d) ST-41, 4 084.5 m; (e) an enlarged view of area C in (d) shows the thin film of crude oil in the pores; (f) pyrite of the Sample ST-50, 4 211.5 m; (g) small droplets of crude oil in Sample ST27, depth 4 036.0 m; (h) small droplets of crude oil in Sample ST10, depth 3 973.2 m; (i) an enlarged view of area D in (f) shows the small droplets of crude oil in the inter-crystalline pores in pyrite of the Sample ST-50, 4 211.5 m.

Table 2 Samples porosity calculated by mercury intrusion and nitrogen adsorption

Sample No.	TOC (%)	Hg intruded volume (cm ³ /g)	Bulk density (g/cm ³)	MICP porosity (%)	N ₂ PORE volume (cm ³ /g)	Total porosity (%)
ST-1	0.76	0.007 5	2.653 8	1.993 4	0.016 0	5.39
ST-8	1.19	0.004 0	2.669 3	1.072 5	0.001 0	1.33
ST-10	1.34	0.002 8	2.678 3	0.751 4	0.002 4	1.39
ST-16	0.61	0.007 1	2.647 7	1.889 2	0.002 0	2.41
ST-18	2.43	0.004 1	2.748 9	1.134 6	0.001 1	1.43
ST-20	2.19	0.004 0	2.669 8	1.074 2	0.002 3	1.68
ST-24	0.79	0.006 9	2.649 7	1.816 3	0.002 2	2.41
ST-30	1.65	0.002 7	2.678 8	0.732 4	0.001 3	1.07
ST-33	4.63	0.003 1	2.673 7	0.831 1	0.001 8	1.31
ST-36	1.64	0.001 4	2.600 3	0.363 8	0.001 4	0.73
ST-43	1.50	0.007 0	2.648 5	1.857 1	0.001 3	2.20
ST-47	1.80	0.006 8	2.650 0	1.797 0	0.001 2	2.12

2015): R_o ranges from 1.1% to 1.3%, with thermal evolution within a condensate oil window, TOC is over 3%, pay zone is over 25 m, micro-fractures are well developed, being overpressure, and porosity is over 4%. Although the criteria for continental shale sweet spots in China are not uniform, the key parameters of marine shale oil can be used for reference for

selection of continental shale sweet spots.

According to the above criteria, no sweet spots have been found in Well ST1H. In Oil Group □ at 4 100–4 200 m, only four criteria have been met: TOC is over 3%, pay zone is over 25 m, micro-fractures are well developed, and being overpressure (Fig. 8). There is no obvious correlation between organic carbon and

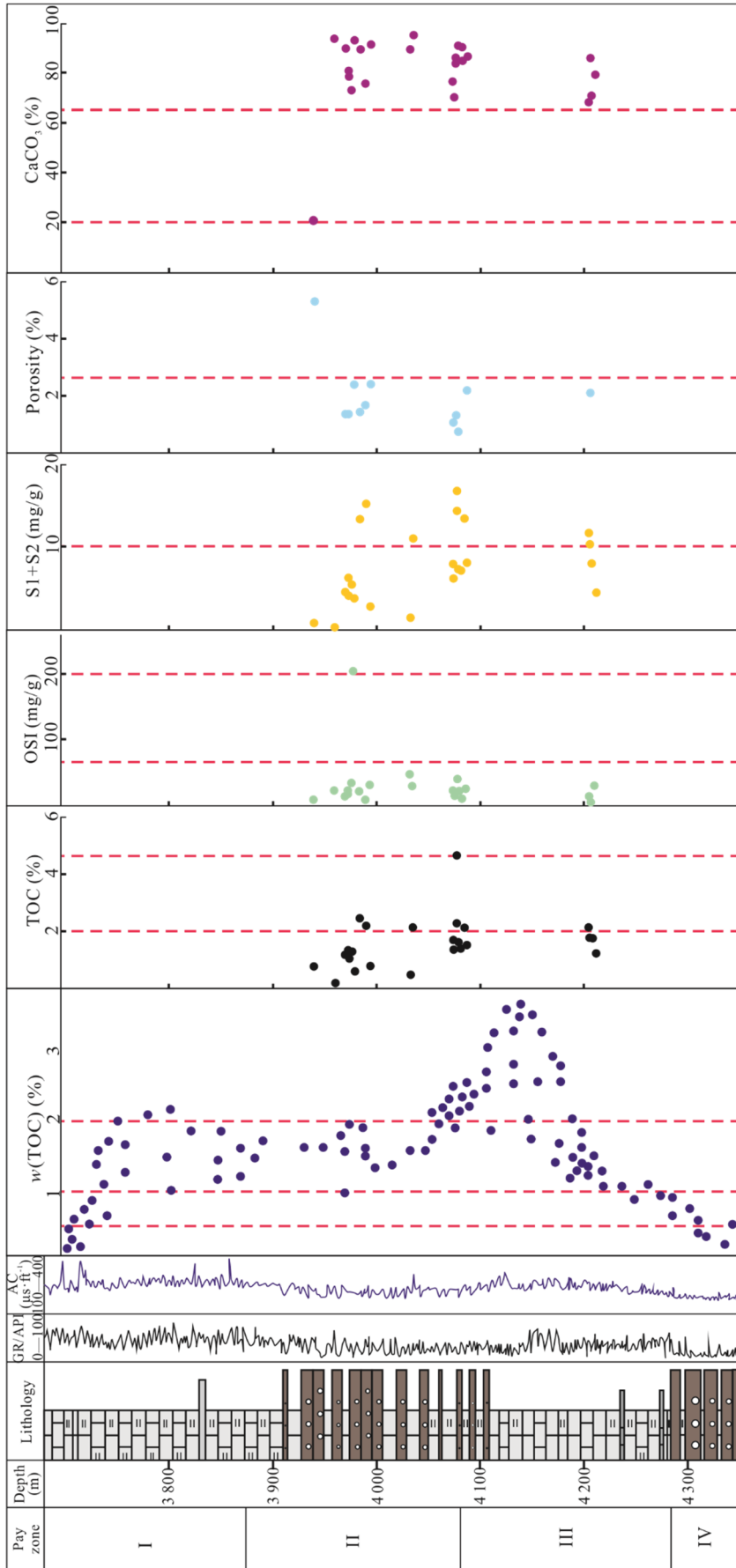


Figure 8. Comprehensive evaluation of sweet spots in Well ST1H.

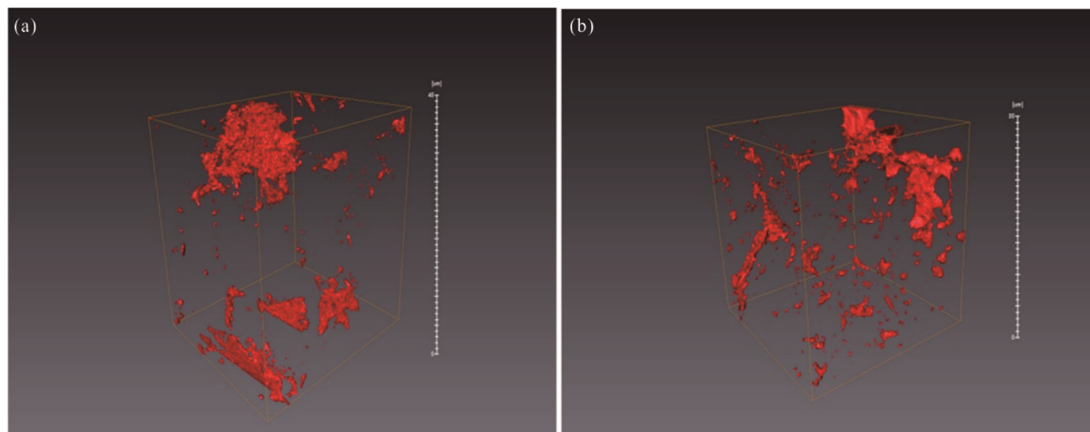


Figure 9. 3D reservoir space in E_{53}^1 samples. (a) Sample ST-16, 3 979.1 m; (b) Sample ST-47, 4 206.3 m.

porosity. This may be the reason for the low maturity of organic matter. Despite this, we still think that rocks with high organic carbon content are favorable horizons as long as the maturity conditions are met (Mendhe et al., 2017).

In the samples from Well ST1H, the porosity is not higher than 4% because the rock is just matured (the average HI=500 mg/g·C). Although good oil /gas shows have been observed, commercial oil production has not been obtained from the marl interval. It is worth noting that based on the OSI Index (oil saturation index) proposed by Jarvie et al. (2007), the OSI Index in the Sample ST-16 is greater than 100, which may be caused by the micro-fractures in the samples. The CT image of the Sample ST-16 indicates that the reservoir space is lamellar, which may be lamellar or micro-fractures (Fig. 9a), and the pore characteristics are clearly different from the dumbbell-shaped pore structure of the III Oil Group in ST-47 (Fig. 9b). Numerous studies have proved that Type \square - \square kerogen organic pores and carbonate pores can increase with the increase of maturity (Wu et al., 2015; Cui et al., 2013). Therefore, we believe that the \square Oil Group is at a lake invasion system where high-quality source rock is well developed, and the controlling factor for sweet spot intervals is the rock maturity. According to the superposition of the marl thickness, formation pressure, organic matter abundance and maturity maps, the potential sweet spot interval is located in the deep buried sag zone.

4 CONCLUSIONS

Through analysis of the mineral composition, geochemical characteristics and pore structures of the E_{53}^1 marl in Sample ST1H, the following conclusions about rock types, pore structures and sweet spots have been obtained:

(1) A four-element classification method has been proposed and seven types of rocks have been identified in the marl in Well ST1H. The primary rocks are medium-high organic carbonate rocks and medium-high organic clayey and siliceous carbonate rocks.

(2) At the marl interval, four types of reservoir spaces have been identified, including intra-granular pores, inter-granular pores (inter-crystalline pores), organic pores, and micro fractures, which are potential effective storage spaces.

(3) According to mercury intrusion and nitrogen adsorption experiments, the porosity of the marl ranges from 0.73% to 5.39%, the distribution of the pore sizes is bimodal, and the pore

types are dominated by micron pores, indicating that the reservoir is low porosity and low permeability reservoir. According to the results of geochemical and reservoir analysis, the III Oil Group may have sweet spot layers.

ACKNOWLEDGMENTS

This study was supported by the National Basic Research Program of China (973 Program) (No. 2014CB239001). Thanks go to Jimao Wang, Yongjun Guo and Zhanwen Yu from the Research Institute of Exploration & Development, PetroChina Huabei Oilfield Company for their help in collecting samples and data. The final publication is available at Springer via <https://doi.org/10.1007/s12583-020-1092-5>.

REFERENCES CITED

- Cao, Z., Liu, G. D., Zhan, H. B., et al., 2016. Pore Structure Characterization of Chang-7 Tight Sandstone Using MICP Combined with N_2 GA Techniques and Its Geological Control Factors. *Scientific Reports*, 6: 36919. <https://doi.org/10.1038/srep36919>
- Chen, S. Y., Zhang, S., Wang, Y. S., et al., 2016. Lithofacies Types and Reservoirs of Paleogene Fine-Trained Sedimentary Rocks in Dongying Sag, Bohai Bay Basin. *Petroleum Exploration and Development*, 43(2): 198–208 (in Chinese with English Abstract)
- Clarkson, C. R., Jensen, J. L., Pedersen, P. K., et al., 2012. Innovative Methods for Flow-Unit and Pore-Structure Analyses in a Tight Siltstone and Shale Gas Reservoir. *AAPG Bulletin*, 96(2): 355–374. <https://doi.org/10.1306/05181110171>
- Clarkson, C. R., Solano, N., Bustin, R. M., et al., 2013. Pore Structure Characterization of North American Shale Gas Reservoirs Using USANS/SANS, Gas Adsorption, and Mercury Intrusion. *Fuel*, 103: 606–616. <https://doi.org/10.1016/j.fuel.2012.06.119>
- Cui, J. W., Zhu, R. K., Cui, J. G., 2013. Relationship of Porous Evolution and Residual Hydrocarbon: Evidence from Modeling Experiment with Geological Constraint. *Acta Geologica Sinica*, 87(5): 730–736 (in Chinese with English Abstract)
- Cui, J. W., Zhu, R. K., Yang, Z., et al., 2015. Progresses and Enlightenment of Overseas Shale Oil Exploration and Development. *Unconventional Oil & Gas*, 2(4): 68–82 (in Chinese with English Abstract)
- Cui, J. W., Li, S., Mao, Z. G., 2019. Oil-Bearing Heterogeneity and Threshold of Tight Sandstone Reservoirs: A Case Study on Triassic Chang7 Member, Ordos Basin. *Marine and Petroleum Geology*, 104: 80–189. <https://doi.org/10.1016/j.marpetgeo.2019.03.028>

- Cui, Z. Q., Guo, Y. J., Li, Y. K., et al., 2015. Calcilutite-Rudstone Petrological Characteristics in the Lower Part of Member 3 of Shahejie Formation, Shulu Sag. *Acta Petrolei Sinica*, 36(S1): 21–30 (in Chinese with English Abstract)
- EIA, 2019. Annual Energy Outlook 2019. <https://www.iea.org/reports/world-energy-outlook-2019>
- Fu, X. D., Wu, J. P., Shou, J. F., et al., 2019. Tight Oil Reservoir Characteristics of Lacustrine Mixed Marlstone in Palaeogene Shahejie Formation of Shulu Sag, Bohai Bay Basin. *Oil & Gas Geology*, 40(1): 78–91 (in Chinese with English Abstract)
- Gregg, S. J., Sing, K. S. W., 1982. Adsorption, Surface Area and Porosity: 2nd ed. Academic Press, London
- Han, C., Tian, J. Z., Zhao, R., et al., 2015. Reservoir Space Types and Its Genesis in Tight Calcilutite-Rudstone Reservoir of the Lower Part of Member 3 of Shahejie Formation, Shulu Sag. *Acta Petrolei Sinica*, 36(S1): 31–39 (in Chinese with English Abstract)
- Jarvie, D. M., Hill, R. J., Ruble, T. E., et al., 2007. Unconventional Shale-Gas Systems: The Mississippian Barnett Shale of North-Central Texas as One Model for Thermogenic Shale-Gas Assessment. *AAPG Bulletin*, 91(4): 475–499. <https://doi.org/10.1306/12190606068>
- Jiang, T., Yang, D. X., Wu, J. P., et al., 2019. Controlling Factors and Patterns of Tight Oil Sweet Spots in Paleogene Lower Es₃ of Shulu Sag of Jizhong Depression, Bohai Bay Basin. *Natural Gas Geoscience*, 30(8): 1199–1211 (in Chinese with English Abstract)
- Jiang, Z. X., Liang, C., Wu, J., et al., 2013. Several Issues in Sedimentological Studies on Hydrocarbon-Bearing Fine-Grained Sedimentary Rocks. *Acta Petrolei Sinica*, 34(6): 1031–1039 (in Chinese with English Abstract)
- Lazar, O. R., Bohacs, K. M., MacQuaker, J. H. S., et al., 2015. Capturing Key Attributes of Fine-Grained Sedimentary Rocks in Outcrops, Cores, and Thin Sections: Nomenclature and Description Guidelines. *Journal of Sedimentary Research*, 85(3): 230–246. <https://doi.org/10.2110/jsr.2015.11>
- Liang, H. B., Kuang, H. W., Liu, J. Q., et al., 2007. Discussion on Origin for Marls of the Member 3 of Shahejie Formation of Paleogene in Shulu Sag of Central Hebei Depression. *Journal of Palaeogeography*, 9(2): 167–174 (in Chinese with English Abstract)
- Li, J., Zhang, P., Lu, S., et al., 2019. Scale-Dependent Nature of Porosity and Pore Size Distribution in Lacustrine Shales: An Investigation by BIB-SEM and X-Ray CT Methods. *Journal of Earth Science*, 30(4): 823–833. <https://doi.org/10.1007/s12583-018-0835-z>
- Li, Q., Jiang, Z. X., You, X. L., et al., 2016. Evaluation of Organic Porosity Based on Its Formation Mechanism: An Example from an Unconventional Marlstone Reservoir in the Shulu Sag, Jizhong Depression. *Geoscience*, 30(2): 394–405 (in Chinese with English Abstract)
- Loucks, R. G., Reed, R. M., Ruppel, S. C., et al., 2009. Morphology, Genesis, and Distribution of Nanometer-Scale Pores in Siliceous Mudstones of the Mississippian Barnett Shale. *Journal of Sedimentary Research*, 79(12): 848–861. <https://doi.org/10.2110/jsr.2009.092>
- Mendhe, V. A., Mishra, S., Khangar, R. G., et al., 2017. Organo-Petrographic and Pore Facets of Permian Shale Beds of Jharia Basin with Implications to Shale Gas Reservoir. *Journal of Earth Science*, 28(5): 897–916. <https://doi.org/10.1007/s12583-017-0779-8>
- Ma, Y. Z., Moore, W. R., Gomez, E., et al., 2016. Wireline Log Signatures of Organic Matter and Lithofacies Classifications for Shale and Tight Carbonate Reservoirs. In: Ma, Y. Z., Holditch, S. A., eds., *Unconventional Oil and Gas Resources Handbook*. Gulf Professional Publishing, Oxford. 164–166. <https://doi.org/10.1016/b978-0-12-802238-2.00005-5>
- Qiu, L. W., Du, R., Liang, H. B., et al., 2006. The Formation of Carbonate Breccia in Shulu Depression. *Acta Sedimentologica Sinica*, 24(2): 202–209 (in Chinese with English Abstract)
- Schmitt, M., Fernandes, C. P., da Cunha Neto, J. A. B., et al., 2013. Characterization of Pore Systems in Seal Rocks Using Nitrogen Gas Adsorption Combined with Mercury Injection Capillary Pressure Techniques. *Marine and Petroleum Geology*, 39(1): 138–149. <https://doi.org/10.1016/j.marpetgeo.2012.09.001>
- Sondergeld, C. H., Ambrose, R. J., Rai, C. S., et al., 2010. Micro-Structural Studies of Gas Shales. In: SPE Unconventional Gas Conference. Pittsburgh, Pennsylvania. 1–9. <https://doi.org/10.2118/131771-ms>
- Song, T., Li, J. Z., Jiang, X. Y., et al., 2013. Features of Marl Tight Oil in Source Rock and Reservoir in Shulu Sag of Central Hebei Depression, Bohai Bay Basin. *Journal of Northeast Petroleum University*, 37(6): 47–54 (in Chinese with English Abstract)
- Tang, X., Zhang, J. C., Jiang, Z. X., et al., 2018. Heterogeneity of Organic-Rich Lacustrine Marlstone Succession and Their Controls to Petroleum Expulsion, Retention, and Migration: A Case Study in the Shulu Sag, Bohai Bay Basin, China. *Marine and Petroleum Geology*, 96: 166–178. <https://doi.org/10.1016/j.marpetgeo.2018.05.031>
- Washburn, E. W., 1921. The Dynamics of Capillary Flow. *Physical Review*, 17(3): 273–283. <https://doi.org/10.1103/physrev.17.273>
- Wu, S. T., Zhu, R. K., Cui, J. G., et al., 2015. Characteristics of Lacustrine Shale Porosity Evolution, Triassic Chang 7 Member, Ordos Basin, NW China. *Petroleum Exploration and Development*, 42(2): 167–176 (in Chinese with English Abstract)
- Yan, J. H., Pu, X. G., Zhou, L. H., et al., 2015. Naming Method of Fine-Grained Sedimentary Rocks on Basis of X-Ray Diffraction Data. *China Petroleum Exploration*, 20(1): 48–54 (in Chinese with English Abstract)
- Yang, C. Q., Sha, Q. A., 1990. Sedimentary Environment of the Middle Devonian Qujing Formation, Qujing, Yunnan Province: A Kind of Mixing Sedimentation of Terrigenous Clastics and Carbonate. *Acta Sedimentologica Sinica*, 8(2): 59–66 (in Chinese with English Abstract)
- Zhang, R. F., Tian, R., Li, M., et al., 2015. Stratigraphic Sequence and Types of Oil and Gas Reservoirs in the Lower Part of Member 3 of Shahejie Formation in Shulu Sag. *Acta Petrolei Sinica*, 36(S1): 10–20 (in Chinese with English Abstract)
- Zhao, X. Y., He, D. B., 2012. Clay Minerals and Shale Gas. *Xinjiang Petroleum Geology*, 33(6): 643–647 (in Chinese with English Abstract)
- Zhao, X. Z., Zhu, J. Q., Zhang, R. F., et al., 2014. Characteristics and Exploration Potential of Tight Calcilutite-Rudstone Reservoirs in Shulu Sag, Jizhong Depression, North China. *Acta Petrolei Sinica*, 35(4): 613–622 (in Chinese with English Abstract)
- Zhao, X. Z., Jiang, Z. X., Zhang, R. F., et al., 2015. Geological Characteristics and Exploration Practices of Special-Lithology Tight Oil Reservoirs in Continental Rift Basins: A Case Study of Tight Oil in Shahejie Formation, Shulu Sag. *Acta Petrolei Sinica*, 36(S1): 1–9, 30 (in Chinese with English Abstract)
- Zhou, L. H., Pu, X. G., Deng, Y., et al., 2016. Several Issues in Studies on Fine-Grained Sedimentary Rocks. *Lithologic Reservoirs*, 28(1): 6–15 (in Chinese with English Abstract)
- Zhu, R. K., Bai, B., Cui, J. W., et al., 2013. Study Advance of Microstructure in Unconventional Tight Oil and Gas Reservoirs. *Journal of Palaeogeography*, 15(5): 615–623 (in Chinese with English Abstract)